Gastrodenol suppresses NLRP3/GSDMD mediated pyroptosis and ameliorates inflammatory diseases

Yunshu Wang
Nanjing University
Peipei Chen
Nanjing University
Sen-lin Ji
Nanjing University
Jing Wang
Nanjing University
Zhuo Liu
Nanjing University
Tingting Wang (wangtt@nju.edu.cn)
Nanjing University
Yun Xu
Nanjing University

Research Article

Keywords: NLRP3 inflammasome, pyroptosis, Gastrodenol, sepsis, experimental autoimmune encephalomyelitis

Posted Date: December 4th, 2023

DOI: https://doi.org/10.21203/rs.3.rs-3682381/v1

Additional Declarations: No competing interests reported.

Abstract

Pyroptosis, a form of inflammatory programmed cell death, plays a pivotal role in the pathogenesis of various diseases. This process is primarily mediated by the nucleotide-binding oligomerization domain-like receptor family pyrin domain-containing protein 3 (NLRP3). Gastrodenol (Bismuth tripotassium dicitrate, GAS) is a mineral compound which is used to treat duodenal and gastric ulcers associated with *Helicobacter pylori*. In this study, GAS was found to exhibit protective effects against classical pyroptosis in macrophages. Specifically, GAS effectively inhibits the activation of the NLRP3 inflammasome, Gasdermin D (GSDMD)-mediated pyroptosis, and the secretion of pro-inflammatory cytokines. Mechanistically, GAS inhibited NLRP3 oligomerization and reduced the oligomerization of adaptor protein apoptosis-associated speck like protein containing a caspase activation and recruitment domain (ASC). In mouse models, GAS treatment demonstrated remarkable attenuation of pyroptosis-mediated inflammatory diseases, including experimental autoimmune encephalomyelitis (EAE) model, lipopolysaccharide (LPS)-induced septic mice, and monosodium urate (MSU)-induced peritonitis. These findings collectively establish GAS as a potent inhibitor of pyroptosis and propose a novel therapeutic strategy for the prevention and treatment of NLRP3-GSDMD mediated diseases.

1. Introduction

NLRP3 inflammasome comprises apoptosis-associated speck-like protein NLRP3, apoptosis-associated speck-like protein containing a caspase-recruitment domain (ASC), and pro-caspase-1[1]. This inflammasome orchestrates the process of pyroptosis, an inflammatory form of programmed cell death. Upon exposure to exogenous or endogenous stimuli, such as pathogen infection and toxins, the assembly of the NLRP3 inflammatory complex is triggered. The NLRP3 inflammasome cleaves procaspase-1 into p20 and p10, leading to the maturation and release of Interleukin-1β (IL-1β) and IL-18[2]. Concurrently, pro-caspase-1 undergoes self-cleavage, resulting in the activation of caspase-1 with enzymatic activity. The activated caspase-1 then cleaves and activates gasdermin D (GSDMD), generating its N-terminus and C-terminus. Subsequently, the N-terminal domain translocates to the cytoplasm[3]. On the cellular membrane, oligomeric pores are formed to trigger cell lysis, thereby releasing cellular contents and pro-inflammatory cytokines such as IL-1β and IL-18, ultimately leading to cell death[4–7]. Under normal circumstances, the activation of the NLRP3 inflammasome is crucial for maintaining tissue equilibrium by eliminating stressed cells and defending against infections through a potent inflammatory response. However, recent discoveries have linked excessive activation of the NLRP3 inflammasome to various diseases, including tumors[8], sepsis[9], multiple sclerosis (MS)[10], and gout[11] etc.

Drugs that inhibit NLRP3 inflammasome activation have shown promise in suppressing the severity and progression of inflammatory diseases, suggesting their potential as therapeutic candidates for inflammasome-related conditions[12]. GAS, a clinical anti-peptic ulcer medication, is commonly used to alleviate discomfort caused by excessive gastric acid, such as gastric ulcer, duodenal ulcer, chronic gastritis, as well as to relieve stomach pain, heartburn, and acid reflux resulting from excessive gastric

acid[13, 14]. However, there is limited research on the anti-inflammatory properties of GAS, and its underlying mechanisms remain unknown. We hypothesize that GAS may inhibit NLRP3 activation and exert a protective effect against inflammasome-related diseases. Given the widespread clinical use of GAS, it is of utmost importance to investigate its impact on NLRP3 inflammasome activation and related animal models.

In this study, we conducted in vitro and in vivo experiments to test this hypothesis. We confirmed that GAS effectively suppressed the activation of the NLRP3 inflammasome in macrophages. Furthermore, GAS demonstrated the ability to alleviate monosodium urate (MSU)-induced peritonitis and reduce clinical scores in experimental autoimmune encephalomyelitis (EAE) mice. It also ameliorated organ damage in septic mice, prolonged their survival time, and mitigated the release of inflammatory factors. Taken together, our data reveals the potential application of GAS as a drug to treat inflammatory diseases associated with NLRP3-GSDMD mediated diseases.

2. MATERIALS AND METHODS

2.1. Reagents and antibodies

GAS (S5866) was brought from Selleck (TX, USA). Adenosine triphosphate (ATP, A6419), nigericin (481990), lipopolysaccharide (LPS, L2630) and phorbol 12-myristate 13-acetate (PMA, P1585) were brought from Sigma-Aldrich (MO, USA). Poly (deoxythymidylic-deoxyadenylic) acid (Poly (dA:dT), 6249-42-01) was brought from Invitrogen (CA, USA). Enzyme-linked immunosorbent assay (ELISA) kits for murine IL-1β (CEK1788), human IL-1β (CEK1731) and antibodies against p-p38 (bs4766), p38 (bs4635), p-C-Jun N-terminal kinase (JNK, bs4322), inhibitor of nuclear factor-kappa B (IκBα, bs3601), p-IκBα (bs4105) were bought from Bioworlde (Nanjing, China). MOG_{35-55} (MEVGWYRSPFSRVVHLYRNGK) was synthesized from Nanjing Peptide Biotech (purity > 99%). Cytotoxicity (LDH) assay kit (C10007), flagellin (P7388) and cell counting kit-8 (CCK-8, C1102) were bought from Beyotime (Shanghai, China). Calcein-AM/Propidium Iodide (PI) (C542) was bought from Dojindo (Shanghai, China). Bicinchoninic acid (BCA) protein assay kit (23225) was brought from Thermo (MA, USA). Fetal bovine serum (FBS, 10091148), opti-Dulbecco's modified Eagle medium (DMEM, 31985-070) and Roswell Park Memorial Institute (RPMI)-1640 (11875119) was bought from Gibico (CA, USA). Antibodies against ASC (CST-67824), glyceraldehyde-3-phosphate dehydrogenase (GAPDH, 5174s), NLRP3 (CST-15101), p-NF-κB (3033s), NF-κB (8242s), p-extracellular signal-regulated kinase (ERK, 4370s), JNK (9258s), were bought from Cell Signaling Technology (MA, USA). Antibodies against IL-1β (AB-401-NA) was bought from R&D Systems (MN, USA). Antibodies against caspase-1 (AG-20B-0042) was bought from Adipogen (CA, USA). Antibodies against ERK (71337) Anti-CD45-PE-Cyanine7 (25-0451-82), Anti-CD11b-Alexa Flour 488 (53-0112-82), Anti-CD4-APC (17-0042-82), Anti-CD8-FITC (11-0081-85), Anti-LY6G-PE (12-5931-81) were bought from eBioscience (CA, USA). Antibodies against IL-1β (AB-401-NA) was bought from R&D Systems (MN, USA). Anti-LY6C-Brilliant Violet 421 (HK1. 4) and Anti-B220-Brilliant Violet 605 (RA3-6B2) were bought from Biolegend (CA, USA).

2.2. Cell culture and stimulation

Exogenous ASC was used to make iBMDMs (RAW264.7-ASC) by injecting it into RAW264.7 macrophages to induce ASC expression. iBMDMs were maintained in DMEM (supplemented with 10% FBS and 1% penicillin-streptomycin). Bone marrow-derived macrophages (BMDMs) were isolated from the hind femora and tibias of C57BL/6 J mice as described previously. BMDMs were cultured in RPMI-1640 (supplemented with 10% FBS and 1% penicillin–streptomycin plus 20% macrophage colony stimulating factor-contained medium from L929 cells) for 6 days. Human monocyte cell line (THP-1, ATCC) cells were cultured in RPMI-1640 (supplemented with 10% FBS and 1% penicilli-streptomycin). 100 nM of PMA was added to THP-1 cells for 16 h to induce macrophage differentiation. All the above cells were cultured at 37°C in a cell culture incubator containing 5% CO_2. iBMDMs and THP-1 cells were primed with LPS (200 ng/mL, 4 h) and then administered GAS, followed by stimulation of NLRP3 activation - nigericin (10 μM, 1 h) or ATP (4 mM, 0.5 h). BMDMs were stimulated with LPS (500 ng/mL, 4 h) before GAS treatment, and finally with nigericin (10 μM, 1 h) or ATP (4 mM, 0.5 h). After treatment with LPS and GAS, iBMDMs were treated with flagellin (2.5 μg/mL, 2.5h), or poly (dA:dT) (1 μg/mL, 6h) to induce NLR family CARD domaincontaining protein 4 (NLRC4) and absent in melanoma 2 (AIM2) inflammasome activation.

2.3. CCK-8 assay

iBMDMs were cultured in 96-well plates at 85–90% density and treated with different concentrations of GAS for 24 h. After incubation, CCK-8 solution was added for 1 h, and the absorbance was measured at 450 nm.

2.4. Western blot analysis

Cells were collected and radio immunoprecipitation assay (RIPA) lysis buffer containing protease inhibitors was added to them. The protein concentration was determined using BCA detection kit. Proteins were separated by sodium dodecyl sulfate-polyacrylamide gel electrophoresis (SDS-PAGE) and electro-transferred to Polyvinylidene difluoride membranes. The membrane was then blocked with skim milk. Following an overnight incubation with a specific primary antibody at 4 ℃ an HRP-conjugated secondary antibody was added to the membrane. Target bands were revealed with high-sig chemiluminescent Western Blotting Substrate (180–5001, Tanon) and blots were recorded.

2.5. LDH Release assay

iBMDMs activated the NLRP3 inflammasome according to the above method and the supernatant was collected. The LDH activity was measured using an LDH detection kit.

2.6. ELISA

Cytokines IL-1β was detected in cell culture supernatants, mouse peritoneal lavage fluid, and mouse serum using ELISA kits following the instructions provided by the manufacturer. The absorbance was measured with microplate reader.

2.7. Cell death assay

Briefly, BMDMs and THP-1 cells were processed using the NLRP3 inflammasome activation protocol described above. PI (3μg/mL) and Calcein AM (2 ng/mL) solutions were added to the PBS to stain dead cells and nuclei, respectively. Cells were incubated at 37℃ for 15 min and 5 fields (BMDMs) or 6 fields (THP-1 cells) were randomly captured by immunofluorescence electron microscopy. The obtained images were processed by Image J.

2.8. ASC oligomerization assay

iBMDMs were cultured in 6-well plates and stimulated with nigericin. Cells were then lysed with NP-40 (containing protease inhibitors) for 30 min. Precipitates in cell lysate were centrifuged at 6000 × g for 15 min at 4°C and incubated with 2 mM disuccinimidyl suberate (DSS) for 30 min at room temperature. Finally, Western blot analysis was performed.

2.9. NLRP3 oligomerization assay

The iBMDM cells were cultured in 6-well plates overnight. After treatment, cells were lyzed with NP-40 lysate which contains protease inhibitors for 30 min, and then centrifuged at 300 g for 5 min to collect the supernatant. The supernatant was added to native gel sample loading buffer. Finally, native-PAGE was performed.

2.10. Mice and animal model

Female C57BL/6J mice (6–8 weeks) were bought from the Model Animal Research Center of Nanjing University (Nanjing, China). Prior to the studies, all the mice had a week of acclimatization. All animal experiments were conducted following the Animal Research: Reporting of In Vivo Experiments guidelines and in accordance with the procedure approved by the Animal Care Committee of Nanjing Drum Tower Hospital.

2.10.1 EAE model

The EAE mouse model was performed essentially as described[15]. C57BL/6J mice (female, 8 weeks) were injected emulsion subcutaneously in the back containing MOG_{35-55} (250μg per mouse), *Mycobacterium tuberculosis* (400μg per mouse) and complete Freund's adjuvant (50μL per mouse). Inject Pertussis toxin (500ng per mouse) intraperitoneally on days 0 and 2. Clinical scores for EAE progression were assessed daily and calculated on a 0–5 scale as follows: 1, tail limp or waddling gait with high tail tension; 2, waddling gait with tail weakness (ataxia); 2.5, ataxia with partial paralysis of a limb; 3, complete paralysis of one limb; 3.5, complete paralysis of one limb and partial paralysis of another limb; 4, complete paralysis of both limbs; 4.5, moribund; 5, death [16]. GAS (10 mg/kg) or vehicle (1% sterile phosphate buffer saline, PBS) was injected intraperitoneally (i.p.) starting on day 0 until the peak stage. Mice were euthanized at the peak stage of EAE disease and perfused with PBS, and the spinal cord and brain were collected. Brain tissue was analyzed by flow cytometry. The spinal cord was subjected to histological staining and real-time quantitative polymerase chain reaction (PCR).

2.10.2 MSU-induced peritonitis model

Mice were treated with GAS (10 mg/kg, i.p.) or vehicle (1% sterile PBS) 24 h before MSU injection. The next day, 1 h after the treatment of GAS or vehicle again, mice were intraperitoneally injected with 1 mg MSU (diluted in sterile PBS) to simulate MSU-induced peritonitis. After 4 h, the mice were anesthetized and sacrificed, and the abdominal cavity was lavaged with 4 ml cold PBS. The peritoneal lavage fluid was centrifuged at 300×g for 10 min at 4°C and the cells and supernatant were collected respectively. The cells were analyzed by flow cytometry and the supernatant was used to measure cytokines by ELISA kits.

2.10.3 Sepsis model

The animal model of sepsis was established by injecting LPS (20 mg/kg, i.p.) into C57BL/6 mice (8 weeks). Mice were given GAS (10 mg/kg, i.p.) or vehicle (1% sterile PBS) intraperitoneally (24 h and 2 h before LPS injection). Survival of mice was recorded every 12 h. Blood samples were collected and analyzed by flow cytometry 12 h after LPS stimulation, and lungs were stained with hematoxylin & eosin (H&E). Serum levels of cytokines IL-1β were measured by ELISA kits.

2.11. Quantitative real-time PCR

Total RNA was extracted using TRIzol and reverse transcribed using the GoScript reverse transcription system. The cDNA was then subjected to real-time PCR using real-time PCR detection system and SYBR Green Master Mix (Vazyme). Relative gene expression levels were determined by the $2^{-\Delta\Delta Ct}$ method, and GAPDH was used as an internal control. The primer sequences are shown in Table 1.

Table 1 Sequences of primers for quantitative PCR

Gene name	Primer sequence	
GAPDH	Forward:	5’-AGGTCGGTGTGAACGGATTTG-3’
	Reverse:	5’-GGGGTCGTTGATGGCAACA-3’
IL-1β	Forward:	5’-AAATACCTGTGGCCTTGGGC-3’
	Reverse:	5’-CTTGGGATCCACACTCTCCAG-3’
IL-6	Forward:	5’-CTGCAAGAGACTTCCATCCAG-3’
	Reverse:	5’-AGTGGTATAGACAGGTCTGTTGG-3’
IL-17	Forward:	5’-CTCCACCGCAATGAAGAC-3’
	Reverse:	5’-CTTTCCCTCCGCATTGAC-3’

2.12. Statistical Analysis

Three independent repeats of each experiment were made. GraphPad Prism 6.0 (GraphPad Software Inc.) was used to analyze the data, which were presented as mean ± standard deviation (SD). To examine the

statistical significance between two groups and among multiple groups, the unpaired Student's t test and one-way analysis of variance (ANOVA) were applied, respectively. Significance was defined as follows: $^{*}P < 0.05$, $^{**}P < 0.01$, $^{***}P < 0.001$, and $^{****}P < 0.0001$.

3. RESULT

3.1. GAS inhibits the activation of NLRP3 inflammasome in mice macrophages

To verify the inhibitory effect of GAS on NLRP3 inflammasome activation, we conducted the following study. First, we determined the cytotoxicity of GAS on iBMDMs using CCK8 Kit. However, we did not find any significant effect of GAS on cell survival after 24 h of incubation (Fig. 1.b). We then induced NLRP3 inflammasome activation with two NLRP3 agonists, including nigericin and ATP. Through this, we investigated whether GAS inhibits the release of IL-1β, a marker of NLRP3 inflammasome activation. As expected, ELISA results of cell supernatants showed that GAS reduced IL-1β release in iBMDMs and BMDMs (Fig. 1.c-f). Similarly, Western Blot results confirmed that GAS inhibited the release of cleaved IL-1β and caspase-1 in the supernatant, but did not reduce the expression levels of pro-caspase-1, pro-IL-1β, and NLRP3 in the cell lysate. (Fig. 1.g-j). The above results indicated that GAS reduced the secretion of IL-1β induced by NLRP3 inflammasome in mice macrophages.

3.2. GAS inhibits GSDMD cleavage and pyroptosis in macrophages

To determine whether GAS could reduce the cleavage of GSDMD, we performed Western Blot on iBMDMs and BMDMs. GSDMD-NT was significantly reduced in the GAS-treated group (Fig. 2.a-d). Furthermore, GAS reduced LDH release (Fig. 2.e-h). GAS blocked GSDMD activation and LDH release, suggesting that GAS inhibited NLRP3 inflammasome-dependent pyroptosis. We also conducted PI/Calcein AM staining. As expected, GAS inhibited pyroptosis in BMDMs (Fig. 2.i-j). Similarly, we verified whether GAS can inhibit the activation of NLRP3 inflammasome and the cleavage of GSDMD in human THP-1 cells, a human-derived cell line. The results showed that GAS reduced the release of IL-1β and inhibited NLRP3 inflammasome-dependent pyroptosis in THP-1 cells (Fig. 3.a-f).

3.3. GAS specifically affects the activation of NLRP3 inflammasome

NF-κB is a key mediator of NLRP3 inflammasome initiation signals by inducing the expression of pro-IL-1β and NLRP3[17]. Western blot showed that GAS didn't inhibit the phosphorylation of IκBα, NF-κB, ERK, JNK, and p38 (Fig. 4.a), indicating that GAS did not affect the NF-κB signaling pathway. To further confirm these findings, we conducted immunoblotting to analyze the core components of the NLRP3 inflammasome, including pro-IL-1β, pro-caspase-1, ASC, and NLRP3. As expected, treatment with GAS did not have any effect on the expression of these proteins (Fig. 4.b). Additionally, we investigated the effects

of GAS on other enzymatic bodies, such as AIM2 and NLRC4. Interestingly, GAS did not affect the activation of AIM2 (Fig. 4.c, e) or NLRC4 (Fig. 4.d, f) immune bodies. Furthermore, GAS did not alter the expression of ASC in cell lysates but inhibited the formation of ASC oligomers, as observed through Western blot analysis (Fig. 4.g). It was also shown that GAS inhibited the oligomerization of NLRP3(Fig. 4.h). Collectively, these results suggest that GAS specifically prevents the assembly of the NLRP3 inflammasome.

3.4. GAS ameliorates LPS-induced septic shock and IL-1β production

In the context of gram-negative bacterial infection, LPS triggers pyroptosis, leading to fatal endotoxemia and sepsis cascade. Remarkably, pretreatment with GAS (10 mg/kg, i.p.) significantly improved the survival rate of septic mice induced by LPS (Fig. 5.a, b) and reduced inflammatory infiltration in the lungs (Fig. 5.c). To further evaluate the effect of GAS treatment on peripheral inflammatory cells, we analyzed mononuclear cells isolated from peripheral blood using flow cytometry. Notably, GAS increased the proportion and cell number of $CD45^+Ly6C^+$ monocytes and $CD45^+CD11b^+Ly6G^+$ neutrophils in peripheral blood of mice (Fig. 5.d, e). Simultaneously, GAS decreased the concentration of IL-1β in the serum (Fig. 5.f). These findings demonstrated that GAS effectively ameliorated LPS-induced septic shock and reduced the production of pro-inflammatory cytokines such as IL-1β.

3.5. GAS inhibits the development of EAE in mice

Multiple sclerosis (MS) is an autoimmune degenerative disease of the central nervous system. In this study, we found that GAS slowed the progression of EAE with a later onset compared with the vehicle group (Fig. 6.b). To evaluate the effects of GAS on CNS, we isolated thoracic spinal cord sections from EAE mice for histological and immunohistochemical evaluation. Consistent with clinical findings, histological analysis showed that spinal cord white matter inflammation and demyelination lesions were significantly reduced with GAS (Fig. 6.c). To further evaluate the effects of GAS treatment on various inflammatory cells in the CNS, we analyzed cells isolated from the mice brains. The percentages of $CD45^+CD4^+$ T cells, $CD45^+CD8^+$ T cells, $CD45^+$ $CD11b^-B220^+$ B cells and the total number of cells also decreased significantly in the GAS group (Fig. 6.d, e). In addition, the expression levels of IL1b, IL6, and IL17a were significantly decreased in the GAS-treated group (Fig. 6.f-h). Taken together, these results suggested that GAS inhibited immune response and attenuated EAE disease severity significantly.

3.6. GAS ameliorates MSU-induced inflammation in a mouse model of acute peritonitis

Intraperitoneal injection of MSU, which is a commonly used mouse model of acute peritonitis, induces NLRP3-dependent inflammation characterized by IL-1β production and massive neutrophil influx into the peritoneal cavity[18]. At 24h and 1h before MSU injection, mice were administered GAS (10 mg/kg, i.p.) or PBS (Fig. 7.a). GAS pretreatment significantly reduced peritoneal lavage fluid IL-1β levels and reduced the frequency of $CD45^+CD11b^+Ly6G^+$ neutrophils compared with the vehicle control group (Fig. 7.b-d). These

data demonstrated that GAS attenuated the activation of the NLRP3 inflammasome and alleviated MSU-induced acute peritonitis in vivo.

4.DISCUSSION

In this study, we aimed to investigate whether GAS inhibits the activation of NLRP3 inflammasomes. To achieve this, we measured the cleavage of GSDMD and the release of IL-1β in vitro using iBMDMs and BMDMs as cellular models for studying NLRP3 inflammasomes[19, 20]. Our findings demonstrated that GAS significantly suppressed macrophage pyroptosis induced by various NLRP3 stimuli, as evidenced by the inhibition of GSDMD cleavage and IL-1β release. Thus, our study unveiled a novel mechanism by which GAS exerted its anti-inflammatory activity through the modulation of NLRP3 inflammasome activation and macrophage pyroptosis.

Sepsis refers to a life-threatening condition characterized by organ dysfunction resulting from a severe infection that triggers an uncontrolled immune response[21]. In sepsis, the release of toxins, such as LPS and mannan, upon infection can bind to intracellular and extracellular receptors, leading to the production of a large quantity of pro-inflammatory cytokine IL-1β[22]. These cytokines activate lymphocytes and the complement system, causing dysfunction and coagulation abnormalities in various organs throughout the host's body. Sepsis is a critical condition with a high fatality rate[23, 24], and it stands as one of the primary causes of death among hospitalized patients worldwide[25]. Traditional anti-infective therapy and supportive care aim to ameliorate the function of failing organs induced by sepsis, but their therapeutic efficacy is limited[26]. In this current investigation, we had discovered that GAS remarkably prolonged the survival duration of septic mice. Of utmost significance, GAS effectively mitigated acute lung injury while concurrently reducing serum levels of inflammatory cytokines, notably IL-1β. These findings suggested that GAS acted as a mediator in inhibiting the NLRP3 inflammasome and pyroptosis, thereby conferring protection against septic organ damage.

Similarly, MS has been strongly associated with cellular focal demise. MS, an autoimmune degenerative disorder of the central nervous system, is characterized by demyelination, neuronal loss, and progressive neurological dysfunction[27]. Investigations have revealed elevated expression levels of several GSDMD pathway-associated proteins, such as caspase-1 and IL-1β, within MS lesions[28, 29]. Moreover, it has been demonstrated that the inhibition of caspase-1 leads to the pyroptosis of microglial cells and oligodendrocytes in EAE which is a classical animal model of MS[30]. In our present study, we observed that GAS decelerated the progression of EAE and significantly diminished inflammatory and demyelinating foci in the spinal white matter. Furthermore, GAS treatment markedly reduced the percentages and total numbers of CD4 + and CD8 + T cells, as well as B cells, while also decreased the expression levels of IL1b, IL6, and IL17a.

Gout, a prevalent inflammatory arthritis in adult humans, arises from chronic hyperuricemia, leading to the deposition of MSU crystals in the joints and periarticular tissues[11, 31]. Activation of the NLRP3 inflammasome by MSU triggers the development of inflammation [18]. In our current investigation, we

observed that GAS significantly diminished the proportion and quantity of neutrophils in mice with MSU-induced peritonitis, accompanied by reduced levels of peritoneal inflammatory cytokines, including IL-1β and IL-6. These findings suggested the potential application of GAS in the treatment of acute gouty arthritis.

A limitation of this study is the lack of positive drugs in the experiment. Previously identified NLRP3-specific inhibitors, such as MCC950, which can serve as positive controls for GAS, need to be further investigated. In addition, for the specific molecular mechanism of NLRP3 inhibition by GAS, we will next conduct relevant experiments to explore.

In conclusion, our study shows that GAS is an inhibitor of NLRP3 inflammasome activation. At the same time, GAS inhibits sepsis, EAE, and MSU-induced peritonitis, highlighting its potential applications in septic shock treatment, multiple sclerosis, and acute gouty arthritis. GAS can be developed to a lead compound for the treatment of NLRP3-mediated diseases and as a versatile tool for pharmacological studies of NLRP3 biology.

Declarations

Author contributions

Y.X. and T.W. designed the project. Y.W., P.C., S-l.J., H.T., J.W. performed the experiments and analyzed the data. Y.W. and S-l.J. wrote the manuscript. Y.X. and T.W. revised the manuscript. All authors have read and approved the final manuscript.

Funding

This research was supported by the National Natural Science Foundation of China (82101417,81920108017, 82130036), the STI2030-Major Projects (2022ZD0211800), Jiangsu Province Key Medical Discipline (ZDXK202216), the Key Research and Development Program of Jiangsu Province of China (BE2020620), and Nanjing Medical Science and technology development Foundation (YKK20061).

Competing interests

All authors have declared no competing interests.

References

1. Fu and Wu. 2023. Structural Mechanisms of NLRP3 Inflammasome Assembly and Activation. *Annu Rev Immunol*. https://doi.org/10.1146/annurev-immunol-081022-021207.
2. Fritz, Ferrero, Philpott and Girardin. 2006. Nod-like proteins in immunity, inflammation and disease. *Nat Immunol*. https://doi.org/10.1038/ni1412.

3. Shi, Gao and Shao. 2017. Pyroptosis: Gasdermin-Mediated Programmed Necrotic Cell Death. *Trends Biochem Sci*. https://doi.org/10.1016/j.tibs.2016.10.004.
4. Rogers, Erkes, Nardone, Aplin, Fernandes-Alnemri and Alnemri. 2019. Gasdermin pores permeabilize mitochondria to augment caspase-3 activation during apoptosis and inflammasome activation. *Nat Commun*. https://doi.org/10.1038/s41467-019-09397-2.
5. Brennan and Cookson. 2000. Salmonella induces macrophage death by caspase-1-dependent necrosis. *Mol Microbiol*. https://doi.org/10.1046/j.1365-2958.2000.02103.x.
6. Ding, Wang, Liu, She, Sun, Shi, Sun, Wang and Shao. 2016. Pore-forming activity and structural autoinhibition of the gasdermin family. *Nature*. https://doi.org/10.1038/nature18590.
7. Li, Ji, Wu, Wu, Cao, Wang, Xu, Li and Zhang. 2023. Identification of D359-0396 as a novel inhibitor of the activation of NLRP3 inflammasome. *Neurochem Int*. https://doi.org/10.1016/j.neuint.2023.105565.
8. Theivanthiran, Yarla, Haykal, Nguyen, Cao, Ferreira, Holtzhausen, Al-Rohil, Salama, Beasley, Plebanek, DeVito and Hanks. 2022. Tumor-intrinsic NLRP3-HSP70-TLR4 axis drives premetastatic niche development and hyperprogression during anti-PD-1 immunotherapy. *Sci Transl Med*. https://doi.org/10.1126/scitranslmed.abq7019.
9. Danielski, Giustina, Bonfante, Barichello and Petronilho. 2020. The NLRP3 Inflammasome and Its Role in Sepsis Development. *Inflammation*. https://doi.org/10.1007/s10753-019-01124-9.
10. Shao, Chen, Shi, Zhou, Wei, Fan, Yang, Wu and Zhang. 2021. Therapeutic potential of the target on NLRP3 inflammasome in multiple sclerosis. *Pharmacol Ther*. https://doi.org/10.1016/j.pharmthera.2021.107880.
11. Dalbeth, Merriman and Stamp. 2016. Gout. *Lancet*. https://doi.org/10.1016/S0140-6736(16)00346-9.
12. Coll, Robertson, Chae, Higgins, Munoz-Planillo, Inserra, Vetter, Dungan, Monks, Stutz, Croker, Butler, Haneklaus, Sutton, Nunez, Latz, Kastner, Mills, Masters, Schroder, Cooper and O'Neill. 2015. A small-molecule inhibitor of the NLRP3 inflammasome for the treatment of inflammatory diseases. *Nat Med*. https://doi.org/10.1038/nm.3806.
13. Alsohaibani, Alquaiz, Alkahtani, Alashgar, Peedikayil, AlFadda and Almadi. 2020. Efficacy of a bismuth-based quadruple therapy regimen for Helicobacter pylori eradication in Saudi Arabia. *Saudi J Gastroenterol*. https://doi.org/10.4103/sjg.SJG_626_19.
14. Kim, Lee, Kim, Sung and Park. 2020. Efficacy and safety of twice a day, bismuth-containing quadruple therapy using high-dose tetracycline and metronidazole for second-line Helicobacter pylori eradication. *Helicobacter*. https://doi.org/10.1111/hel.12683.
15. Barclay and Shinohara. 2017. Inflammasome activation in multiple sclerosis and experimental autoimmune encephalomyelitis (EAE). *Brain Pathol*. https://doi.org/10.1111/bpa.12477.
16. Yang, Jiang, Fitzgerald, Ma, Yu, Li, Zhao, Li, Ciric, Curtis, Rostami and Zhang. 2009. Adult neural stem cells expressing IL-10 confer potent immunomodulation and remyelination in experimental autoimmune encephalitis. *J Clin Invest*. https://doi.org/10.1172/JCI37914.

17. Zhang, Wang, Wang, Cheng, Xu, Pei, Wang, Fu, Jiang, He and Wei. 2022. Signaling pathways and targeted therapy for myocardial infarction. *Signal Transduct Target Ther*. https://doi.org/10.1038/s41392-022-00925-z.
18. Desai, Steiger and Anders. 2017. Molecular Pathophysiology of Gout. *Trends Mol Med*. https://doi.org/10.1016/j.molmed.2017.06.005.
19. Li, Ji, Qin, Kang, Sun, Wang, Chang, Wang, Zhang, Zou, Nel and Xia. 2014. Interference in autophagosome fusion by rare earth nanoparticles disrupts autophagic flux and regulation of an interleukin-1beta producing inflammasome. *ACS Nano*. https://doi.org/10.1021/nn505002w.
20. Li, Fu, Zhang, Zhou, Yang, Cao, Chen, Tan and Hu. 2021. Overproduction of Gastrointestinal 5-HT Promotes Colitis-Associated Colorectal Cancer Progression via Enhancing NLRP3 Inflammasome Activation. *Cancer Immunol Res*. https://doi.org/10.1158/2326-6066.CIR-20-1043.
21. Singer, Deutschman, Seymour, Shankar-Hari, Annane, Bauer, Bellomo, Bernard, Chiche, Coopersmith, Hotchkiss, Levy, Marshall, Martin, Opal, Rubenfeld, van der Poll, Vincent and Angus. 2016. The Third International Consensus Definitions for Sepsis and Septic Shock (Sepsis-3). *JAMA*. https://doi.org/10.1001/jama.2016.0287.
22. Palsson-McDermott and O'Neill. 2004. Signal transduction by the lipopolysaccharide receptor, Toll-like receptor-4. *Immunology*. https://doi.org/10.1111/j.1365-2567.2004.01976.x.
23. Hotchkiss, Monneret and Payen. 2013. Sepsis-induced immunosuppression: from cellular dysfunctions to immunotherapy. *Nat Rev Immunol*. https://doi.org/10.1038/nri3552.
24. Shi, Zhao, Wang, Gao, Ding, Li, Hu and Shao. 2014. Inflammatory caspases are innate immune receptors for intracellular LPS. *Nature*. https://doi.org/10.1038/nature13683.
25. Evans, Rhodes, Alhazzani, Antonelli, Coopersmith, French, Machado, McIntyre, Ostermann, Prescott, Schorr, Simpson, Wiersinga, Alshamsi, Angus, Arabi, Azevedo, Beale, Beilman, Belley-Cote, Burry, Cecconi, Centofanti, Coz Yataco, De Waele, Dellinger, Doi, Du, Estenssoro, Ferrer, Gomersall, Hodgson, Moller, Iwashyna, Jacob, Kleinpell, Klompas, Koh, Kumar, Kwizera, Lobo, Masur, McGloughlin, Mehta, Mehta, Mer, Nunnally, Oczkowski, Osborn, Papathanassoglou, Perner, Puskarich, Roberts, Schweickert, Seckel, Sevransky, Sprung, Welte, Zimmerman and Levy. 2021. Surviving sepsis campaign: international guidelines for management of sepsis and septic shock 2021. *Intensive Care Med*. https://doi.org/10.1007/s00134-021-06506-y.
26. Marshall. 2014. Why have clinical trials in sepsis failed? *Trends Mol Med*. https://doi.org/10.1016/j.molmed.2014.01.007.
27. Wang, Li, Xu and Zhang. 2023. The gut microbiota and associated metabolites in multiple sclerosis. *Advanced Neurology*. https://doi.org/10.36922/an.413.
28. Inoue and Shinohara. 2013. NLRP3 Inflammasome and MS/EAE. *Autoimmune Dis*. https://doi.org/10.1155/2013/859145.
29. Lin and Edelson. 2017. New Insights into the Role of IL-1beta in Experimental Autoimmune Encephalomyelitis and Multiple Sclerosis. *J Immunol*. https://doi.org/10.4049/jimmunol.1700263.

30. McKenzie, Mamik, Saito, Boghozian, Monaco, Major, Lu, Branton and Power. 2018. Caspase-1 inhibition prevents glial inflammasome activation and pyroptosis in models of multiple sclerosis. *Proc Natl Acad Sci U S A*. https://doi.org/10.1073/pnas.1722041115.

31. Mulay and Anders. 2016. Crystallopathies. *N Engl J Med*. https://doi.org/10.1056/NEJMra1601611.

Figures

Fig. 1

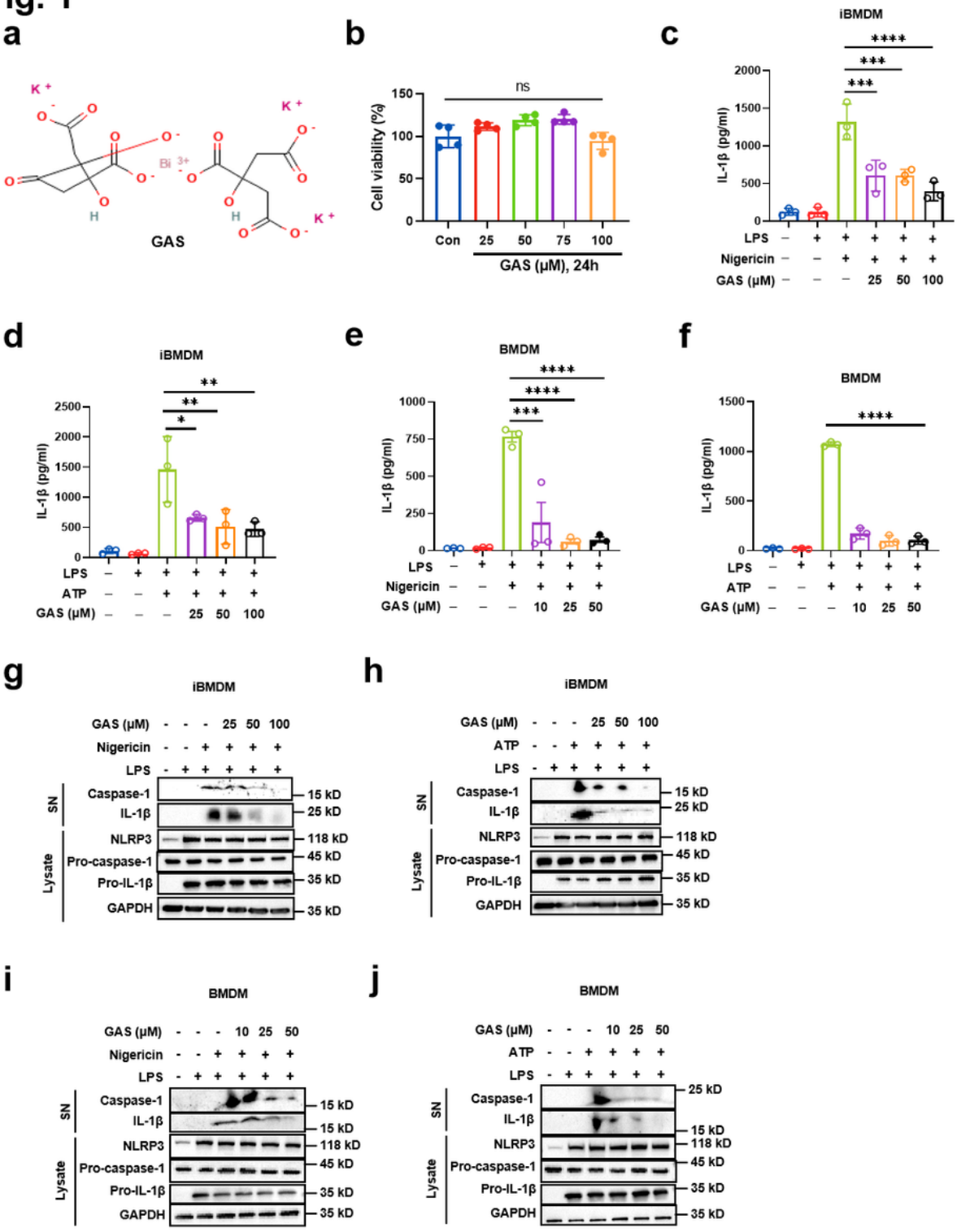

Figure 1

GAS inhibits the activation of NLRP3 inflammasome in mice macrophages

(a) The structure of GAS.

(b) iBMDMs were treated with GAS (25 μM, 50 μM, 75 μM, and 100 μM) for 24 h. CCK-8 was used to assess the vitality of iBMDMs, and the results were standardized to control cell viability.

(c–f) LPS-primed iBMDMs and BMDMs were treated with GAS for 1 h and then stimulated with ATP (C, E), nigericin (D, F) for 1 h. ELISA was used to measure the concentration of IL-1β in the supernatants (SNs).

(g–j) The levels of pro-IL-1β, pro-caspase-1, and NLRP3 in cell lysates and IL-1β, caspase-1 in supernatants from iBMDMs (G, H) or BMDMs (I, J) were determined via Western blot.

Data are representative of n=3 (E) and are expressed as mean±standard error of the mean (SEM). Data are representative of n=4 (B) or n=3 (C, D, F) and are expressed as mean ± SD. *P < 0.05, **P < 0.01, ***P <0.001, ns: not significant.

Fig. 2

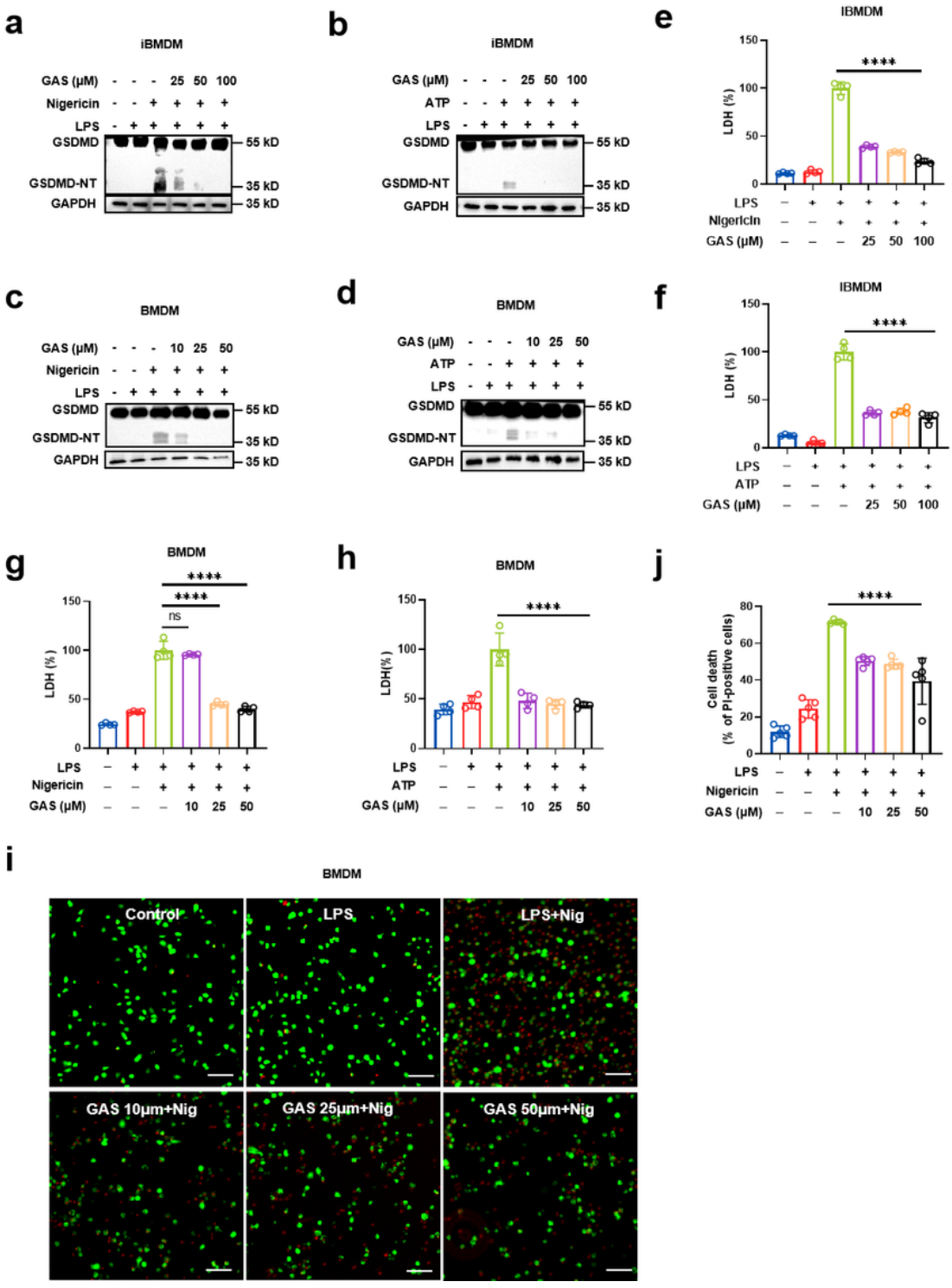

Figure 2

GAS inhibits GSDMD cleavage and pyroptosis in macrophages

(a-d) LPS-primed iBMDMs (A, B) and BMDMs (C, D) were treated with GAS for 1 h and then stimulated with ATP or nigericin for 1 h. Western blot analysis of the expression of GSDMD and cleaved GSDMD-NT in cell lysates.

(e-h) LDH release in the cell supernatants was used to assess cell death.

(i) Representative images of live cells and dead cells detected by immunofluorescence after LPS-primed BMDMs were incubated with GAS for 1 h and then stimulated with nigericin. Scale bar, 100 μm.

(j) The percentage of dead cells in total cells shown in I.

Data are representative of n=4 (E-H) or n=5 (J) and are expressed as mean±SD. *P < 0.05, **P < 0.01, ***P <0.001, ****P <0.0001, ns: not significant.

Fig. 3

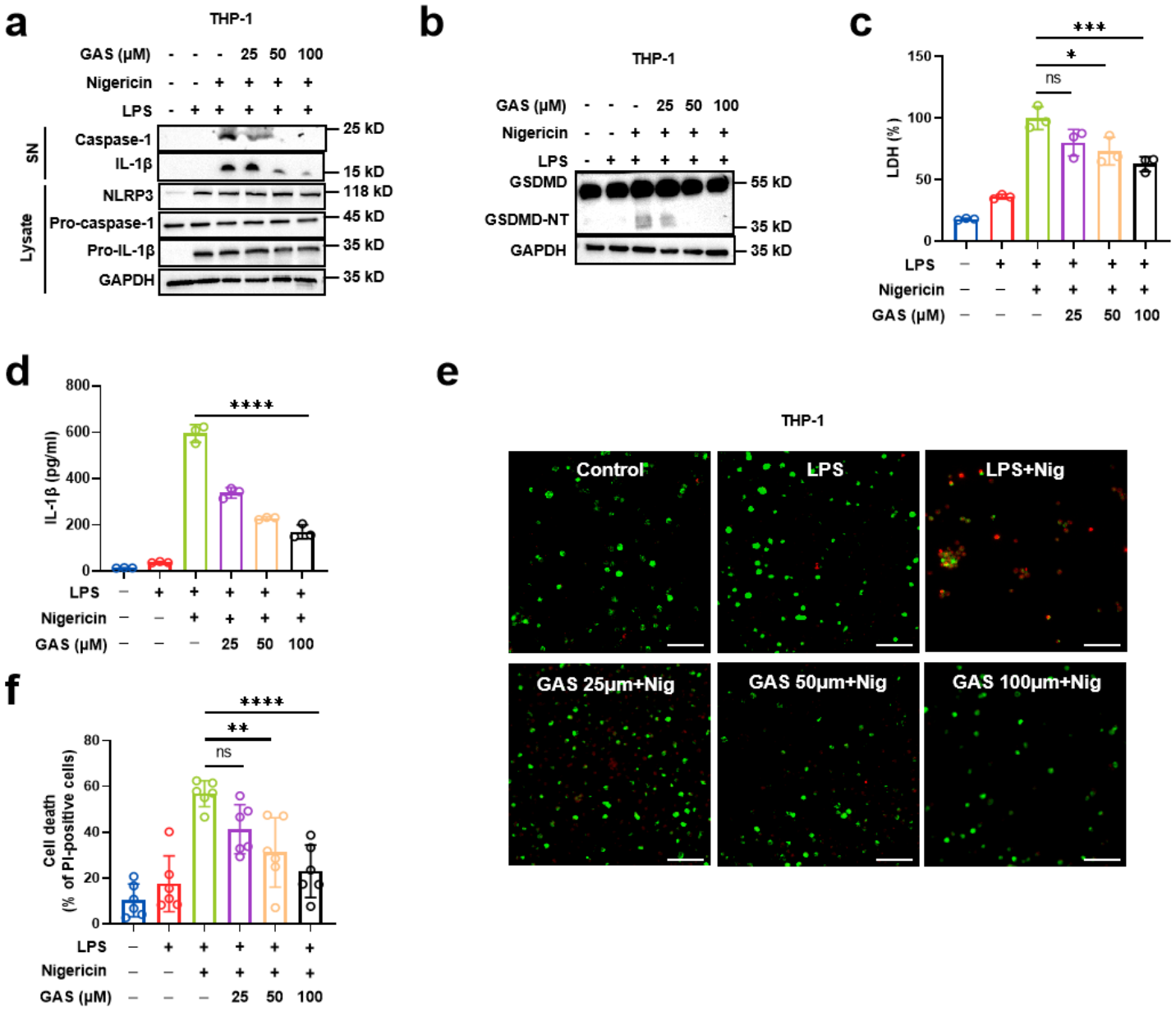

Figure 3

GAS inhibits the activation of NLRP3 inflammasome in human macrophages

(a) LPS-primed THP-1 cells were treated with GAS for 1 h and then stimulated with nigericin for 1 h. Western blot analysis of the expression of pro-IL-1β, pro-caspase-1, and NLRP3 in cell lysates and IL-1β, caspase-1 in SNs.

(b) Western blot analysis of the expression of GSDMD and cleaved GSDMD-NT in cell lysates.

(c) LDH release in the cell supernatants was used to assess cell death.

(d) ELISA was used to measure the concentration of IL-1β in the SNs.

(e) Representative images of live cells and dead cells detected by immunofluorescence after LPS-primed THP-1 cells were incubated with GAS for 1 h and then stimulated with nigericin. Scale bar, 100 μm.

(f) The percentage of dead cells in total cells shown in F.

Data are representative of n=4 (C), n=3 (D) or n=6 (F) and are expressed as mean±SD. *P < 0.05, **P < 0.01, ***P <0.001, ****P <0.0001, ns: not significant.

Fig. 4

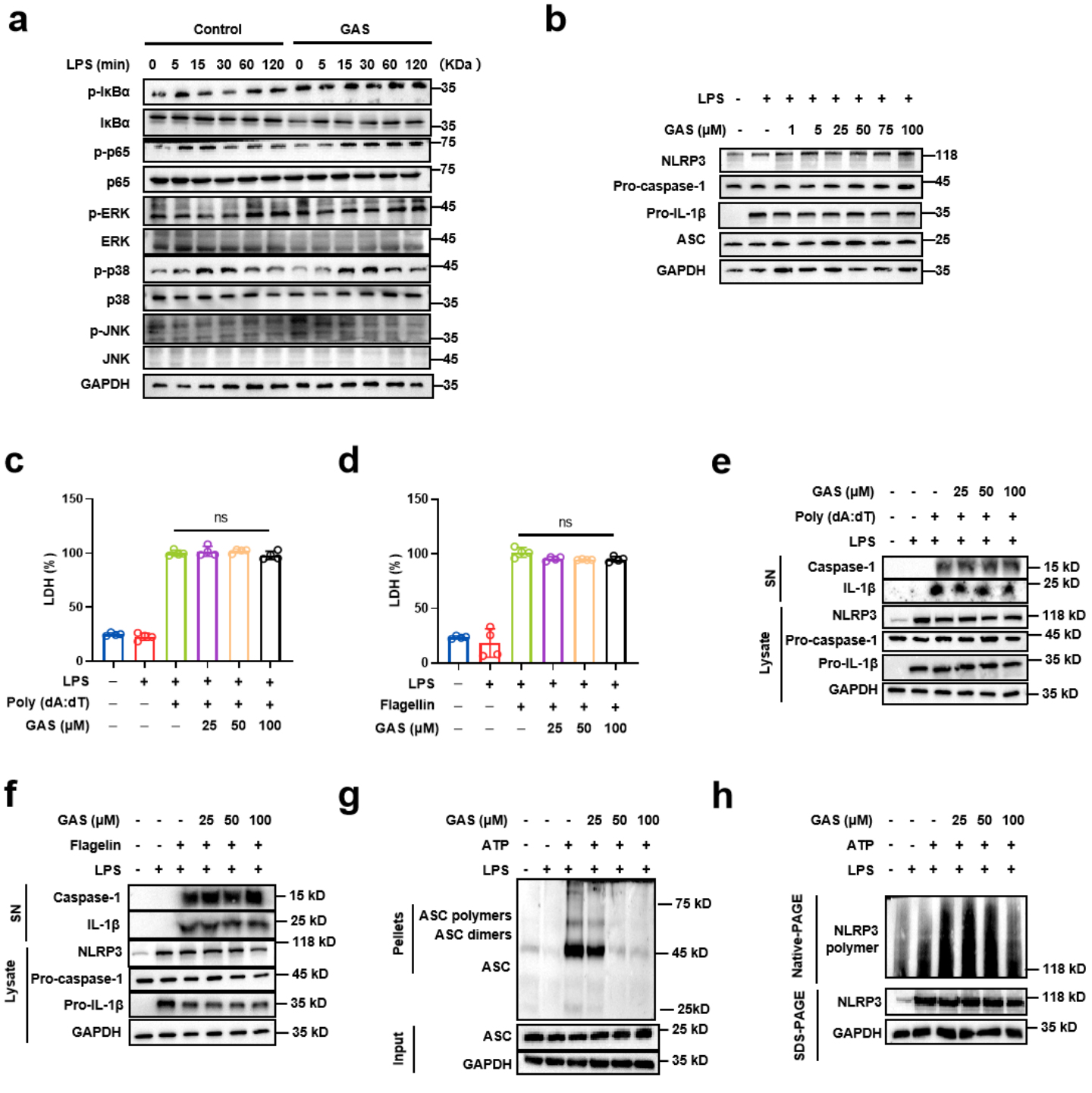

Figure 4

GAS attenuates inflammation independent of NF-κB, ERK, JNK and P38 signaling, but inhibits the assembly of NLRP3 inflammasome

(a) iBMDMs were pretreated with 100 μM GAS along with multiple stimulations of LPS. Western blot analysis of the expression of IκBα, NF-κB, ERK, p38 and JNK.

(b) iBMDMs were pretreated with 100 μM GAS followed by stimulation with LPS for 4 hours. Western blot analysis of the protein expression of NLRP3, pro-caspase-1, pro-IL-1β and ASC.

(c, d) LPS-primed iBMDMs were incubated with GAS for 1 h and then stimulated with Poly (dA: dT) (C) or flagellin (D) for 14 h. Cell death was evaluated by detecting LDH release in cell supernatants.

(e, f) Western blot analysis of the protein expression of pro-IL-1β, pro-caspase-1, and NLRP3 in cell lysates and IL-1β, caspase-1 in SNs.

(g) Western blot analysis of DSS-cross-linked ASC oligomers in the NP-40-insoluble pellet from iBMDMs.

(h) Oligomerization of NLRP3 was measured by the native-PAGE analysis.

Data are representative of n=4 (C, D) and are expressed as mean±SD. ****P <0.0001.

Fig. 5

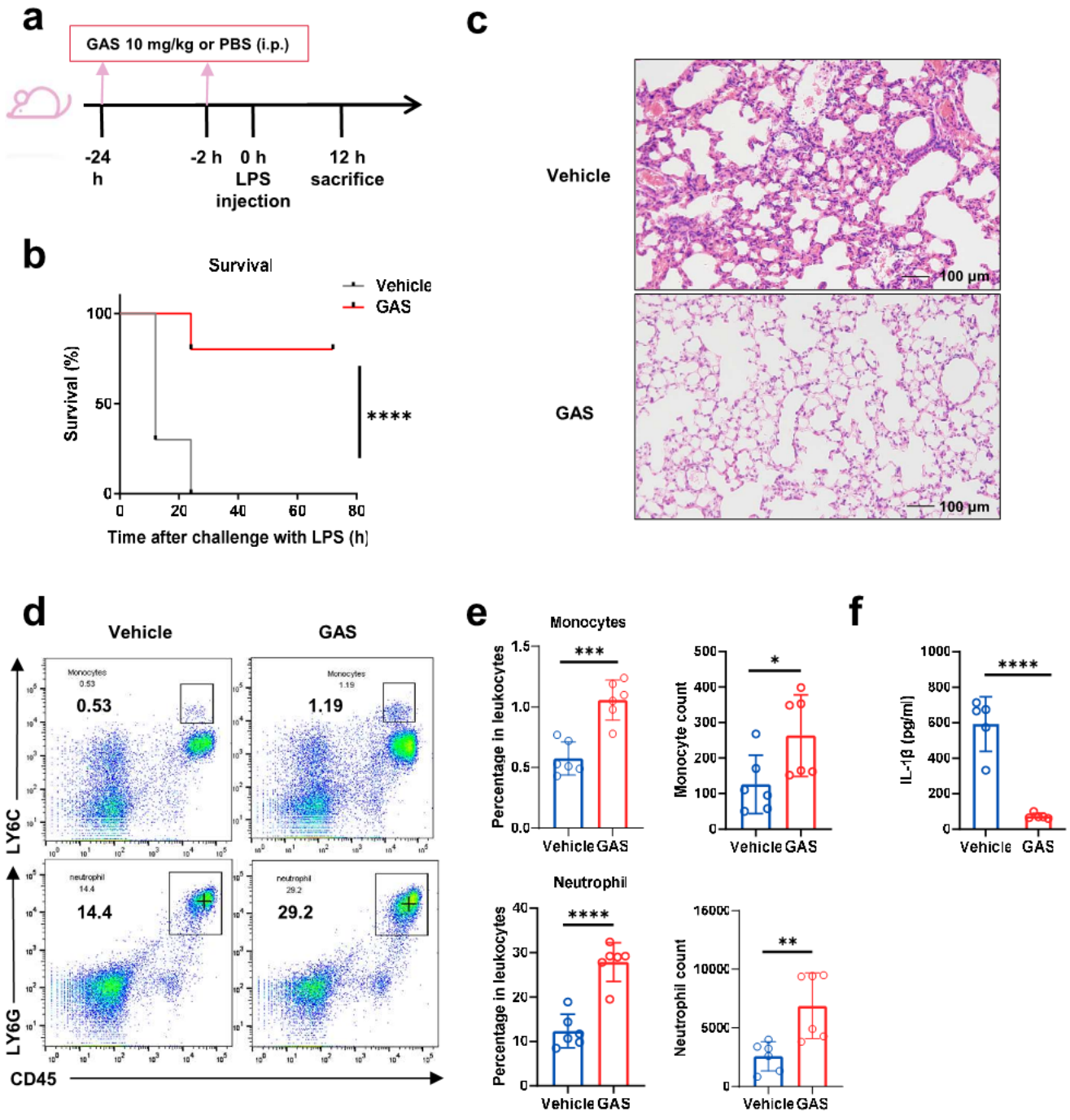

Figure 5

GAS ameliorates LPS-induced septic shock and IL-1β production

(a) C57BL/6 mice were given GAS (10 mg/kg) or PBS at 24 h and 2 h before LPS injection.

(b) After being challenged with 20 mg/kg LPS, the survival rate of mice was monitored every 6 h until 72 h.

(c) Samples of lung tissue encased in paraffin underwent H&E staining. Representative histology pictures are displayed. Scale bar, 100 μm.

(d) Analysis of immune cells by flow cytometry in whole blood from septic mice 12 h after LPS injection (including CD45+LY6C+ monocytes and CD45+CD11b+LY6G+ neutrophils).

(e) Percentage and cells count of $CD45^{+}LY6C^{+}$ monocytes and $CD45^{+}CD11b^{+}LY6G^{+}$ neutrophils.

(f) The serum concentrations of IL-1β were measured via ELISA kits 6 h after LPS injection.

Statistical analysis of the survival rate was performed using the log-rank (Mantel-Cox) test (n=10). Data are representative of n=6 (E) and n=5 (F) and are expressed as mean±SD. *P < 0.05, **P < 0.01, ***P <0.001, ****P <0.0001 vs Vehicle.

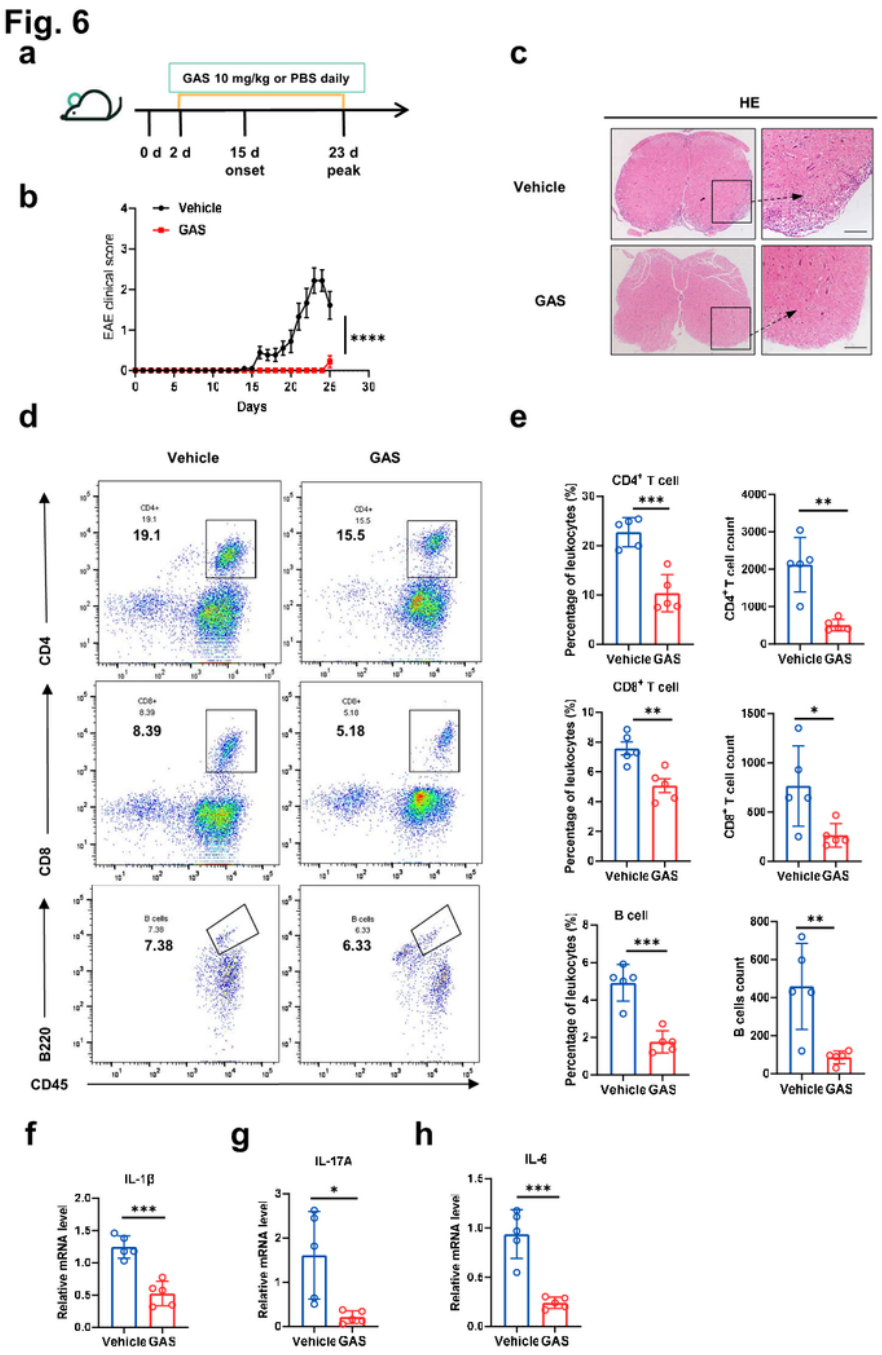

Figure 6

GAS inhibits the development of EAE in mice

(a) EAE was induced in C57BL/6 female mice and treated with intraperitoneal injections of GAS (10 mg/kg), or PBS, starting on day 2 after immunization.

(b) Two researchers conducted daily blind evaluations of EAE development based on a 0–5 scale.

(c) H&E was used to examine thoracic spinal cord slices for signs of inflammation. Scale bar, 300 μm.

(d) Cells from brains were analyzed by flow cytometry on Day 25 (including $CD45^+CD4^+$ T cells, $CD45^+CD8^+$ T cells, $CD45^+CD11b^-B220^+$ B cells).

(e) Percentage and cell count of $CD45^+CD4^+$ T cells, $CD45^+CD8^+$ T cells, $CD45^+$ $CD11b^-B220^+$ B cells.

(f-h) Real-time PCR reaction analysis of IL-1β, IL-17A and IL-6 mRNA levels (normalized to GAPDH levels, n=5 per group).

Data are expressed as mean±SEM and n=9 mice in each group (B). Data are representative of n=5 (E-H) and are expressed as mean±SD. *P < 0.05, **P < 0.01, ***P <0.001, ****P <0.0001 vs Vehicle.

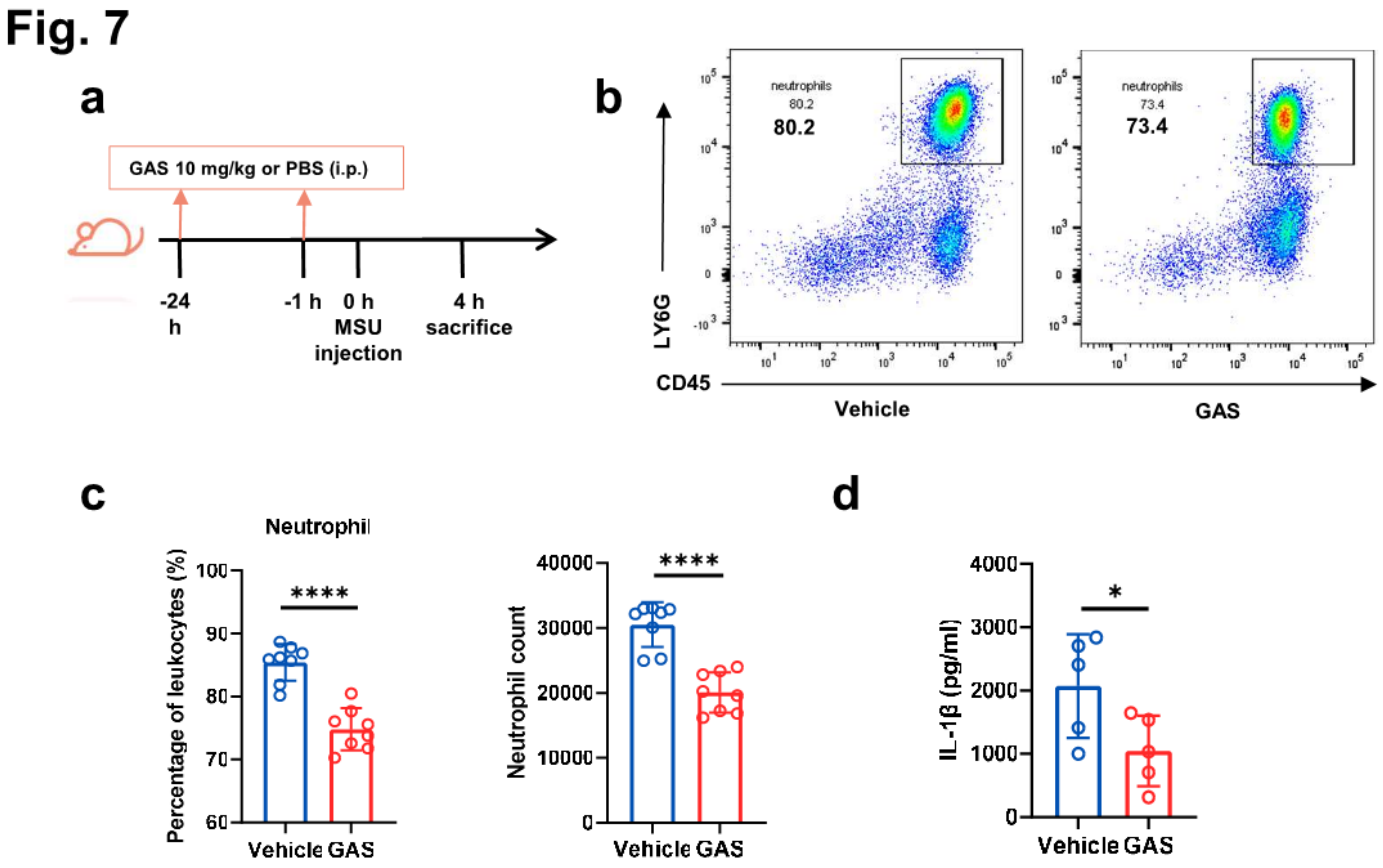

Figure 7

GAS ameliorates MSU-induced peritonitis

(a) C57BL/6 mice were given GAS (10 mg/kg) or PBS 24 h and 1 h before MSU injection.

(b) The representative flow cytometric dot plots of $CD45^+CD11b^+LY6G^+$ neutrophils in peritoneal lavage fluid.

(c) $CD45^+CD11b^+LY6G^+$ neutrophils' percentage and cell count in the peritoneal lavage fluid.

(d) IL-1β levels in peritoneal lavage fluid were measured by ELISA kit.

Data are representative of n=8 (C) and n=5 (D) are expressed as mean±SD. *P <0.05, ***P <0.001, ****P <0.0001 vs Vehicle.